CrossMark

ORIGINAL ARTICLE

Intra-specific relationship between vessel length and vessel diameter of four species with long-to-short species-average vessel lengths: further validation of the computation algorithm

Mengmeng Liu[1] · Ruihua Pan[1] · Melvin T. Tyree[1]

Abstract

Key message **Within a species, vessel length is a linear function of vessel diameter; this suggests that in future, concepts about vessel size optimization need to be revised.**

Abstract This study extends the previous reports that vessel length is a linear function of vessel diameter. Strong relationships were revealed in the wide-vessel species known to have long average vessel lengths. The method used was to reveal the length of cut open vessels by the injection of rubber polymers mixed with ultraviolet sensitive dyes prior to injection and polymerization. Following injection and polymerization, the diameter of every vessel containing rubber was measured at different distances from the injection surface. Then, these values were divided into vessel diameter size classes; the number of vessels in each bin size was used to assess vessel length. Vessel length and diameter were measured in current year stems of *Acer, Populus, Vitis,* and *Quercus* representing short-vessel-to-long-vessel species. Our results showed that the wider vessels were also longer vessels. In addition, mean vessel diameter of rubber-injected vessels increased with distance

Communicated by H. Gaertner.

Mengmeng Liu and Ruihua Pan have contributed equally to this study.

✉ Melvin T. Tyree
  mel.tyree@cantab.net

1 College of Forestry, Northwest A&F University, Yangling 712100, Shaanxi, China

from the injection surface. If vessel diameter changed randomly over the length of individual vessels, then the correlations in the previous two sentences would not exist.

Introduction

Vessel length is an extremely important hydraulic trait, because it relates to the hydraulic efficiency of vessel. Hydraulic efficiency depends both on vessel diameter, D, and vessel length, L, because, according to Poiseuille's law, the hydraulic conductance of a pipe is proportional to D^4/L, where conductance gives the proportionality between flow and pressure drop in a pipe. Overall efficiency of transport depends on a balance between conductance of conduit lumens and end wall conductance which is a function of pit area, A_P, in contact between vessels. However, there can be negative consequences associated with hydraulic efficiency, because the hydraulic advantage of big vessels might be at the cost of increased vulnerability to cavitation (Cai and Tyree 2010).

Two measuring methods are normally used in vessel length determination. One is the rubber-injection method (Pan et al. 2015), which involves injection of rubber while still in the liquid (non-polymerized) state. The rubber polymers are small enough to pass through vessels but too large to pass through pit membranes. After the rubber-injection process, the polymer chains cross-link to form a solid rubbery mass. The average vessel length is calculated by analysis of the number of rubber-filled vessels at various distances away from the injection surface. Another

common technique is the air injection method (Pan et al. 2015). Air is injected into stem segments while measuring the air flow rate out of the cut surface distal of the air injection surface. If the segment is longer than the longest vessel, then no air passes through, because the wet pit membranes prevent air flow. The air flow rate increases as the stem segment is cut into progressively shorter lengths, because more vessels are cut open at both ends as the segment is shortened. The air injection method is much faster than the rubber injection. The air injection method is fast enough to permit the measurement of five or more stems per day, whereas the rubber-injection method requires at least 80 h of work to measure five stems. The rubber-injection method provides information about many parameters about vessels; the extra information to be gained by the rubber-injection method may be worth the extra time required to obtain the information.

The relationship between vessel length and vessel diameter has been examined over recent years. The earliest studies focused on mean vessel length, $\bar{L}$, and the mean vessel diameter, $\bar{D}$, of a species and the functional dependence of $\bar{L}$ versus $\bar{D}$ between species (Hacke et al. 2006; Jacobsen et al. 2012; Sperry et al. 2007). For example, Hacke et al. (2006) found that there was a functional relationship of $\bar{L}$ versus $\bar{D}$ between 29 species (vine, ring-porous, and diffuse-porous tree, and shrub).

It has been recognized for many years that $\bar{L}$ represents the mean of a specific distribution of vessel lengths. Cohen et al. (2003) derived the following probability distribution for vessel length from his empirical results:

$$P_x = x\lambda_v^2 \exp(\lambda_v x), \tag{1}$$

where P_x is the probability distribution function (PDF), x is the length, and λ_v is a negative constant. Subsequently, Cohen (personal communication) identified Eq. (1) as equivalent to a gamma distribution with parameters $(2, \lambda)$, where 2 is a shape parameter. The PDF in Eq. (1) has the property that the mode vessel length $= -1/\lambda_v$ and the mean of vessel length $= -2/\lambda_v$.

More recently, Cai et al. (2010) extended the analysis algorithm to come up with a way of determining how vessel length, L_v, is a function of vessel diameter, D_v, within a species. The new algorithm for analysis used the rubber-injection method, but differed in that the number of vessels was divided into bin diameter size classes, D_{bin}. Counts of vessels within each D_{bin} were then used in Eq. (1) to yield information on how L_v depended on value of D_v in the center of each bin diameter size class. This new analysis algorithm was applied to three species of *Populus* (Cai et al. 2010) to find information about the dependence of L_v on D_v within each of three *Populus* species or clones. To be specific, the wider vessels were

longer vessels within *Populus* species. So far, we are aware of no other studies that expand the algorithm to other taxa regarding the dependence of L_v versus D_v. Our hypothesis was that a wide range of species might display the patterns observed in Cai's research.

The analysis of Cai et al. (2010) assumed that D_v remains approximately constant over the entire vessel length and that long vessels had higher D_v values than short vessels. If this is true, then an additional prediction is that average vessel diameter of rubber-injected vessels should increase with increasing distance from the injection surface. The two weaknesses of the analysis of Cai et al. (2010) were that (1) they did not prove that vessel diameter of rubber-injected vessels increased with distance from the injection surface, and (2) the range of vessel widths and lengths were quite limited in Cai et al. (2010) making the conclusions somewhat unconvincing. This study will redress these two weaknesses.

The readers should note that the null hypothesis has quite different consequences. For example, if vessel diameter varies 'randomly' over the entire vessel length, then there should be no dependence of L_v on D_v, and also the mean vessel diameter should be a constant value independent of the distance from the injection point where it is measured. Or if all vessels were the same length regardless of diameter, then the analysis in this paper should reveal that fact.

The above ideas would not be tested with the original data set of Cai et al. (2010) because of the insufficient range of L_v on D_v. Therefore, in this study, a range of species were selected with a wide range of vessel dimensions from long- to short-vessel lengths and wide- to narrow- vessel diameters.

Methods

Plant material

The study included four species: *Acer truncatum* Bunge, the '84K' *Populus* hybrid clone (*Populus alba* L. × *Populus glandulosa* Uyeki), *Vitis vinifera* L.cv Cabernet Sauvignon, and *Quercus variabilis* Bl. The species are listed in order from smallest to largest mean vessel length and will hereafter be referred to as *Acer, Populus, Vitis,* and *Quercus. Acer* and *Populus* were collected in March 2015 before the commencement of the spring growth; *Vitis* and *Quercus* were sampled in September 2015, about a month before the normal fall shedding of leaves, so that the current growth ring had reached maximum development for the growth year. All experiments were done on the current year stems for all

four species. The samples were collected from the campus of Northwest A&F University. Stem segments were excised from terminal shoots; the excised shoots with a basal diameter of about 10 mm (including bark) were excised in the morning and put into a black plastic bag after spraying the leaves with water. Samples were brought back to a laboratory within 20 min. After immersion of the shoots in water, smaller stem segments 40 cm long and 6–7 mm basal diameter were subsampled.

Silicone rubber injection

Stems were flushed with 10 mM KCl solution at 1.5 bar for 30 min to remove air bubbles in vessels that would interfere with the injection of silicone rubber fluid, and were injected with un-polymerized liquid rubber made up of parts 'A' and 'B' in the ratio of 10:1, i.e., 10 g RTV141 part A mixed with 1 g of RTV141 part B (Rhodorsil RTV-141; Rhodia USA, Cranbury, NJ, USA; imported by Walco Materials, Escondido, CA, USA). Uvitex (OB, Samwon Industrial Co., Ltd., Ansan Gyeonggi-do, Korea), a fluorescent optical brightener, was dissolved in chloroform (1% w/w) and added to the mixed silicone rubber at the ratio of 1:40 to make the silicone rubber visible under UV light. The stems were injected with silicone at 1.5 bar for 24 h, and then, the silicone was hardened for 12 h in an oven at 38 °C while immersed in water to prevent wood drying (Cai et al. 2010).

The cured stems were cross-sectioned at several distances from the injection surface. *Acer* was sectioned at 0.2, 0.5, 1, 1.5, 2, 3, and 4 cm, and *Populus* was sectioned at 0.2, 0.5, 1, 1.5, 2, 4, 6, and 8 cm; *Vitis* was sectioned at 0.2, 1, 2, 6, 9, 12, 18, and 22 cm; *Quercus* was sectioned at 0.2, 1, 2, 4, 8, 16, 24, and 28 cm. The distances used for sampling were determined from preliminary measurements of vessel length by air injection.

Image capture

A microtome (Reichert-Jung 2030 Biocut; Leica, Heidelberg, Germany) was used to cut 20 μm thick cross sections from rubber-filled stems. These intact sections were mounted in glycerin on a glass slide and placed on a microscope (Zeiss Axioskop 40; Carl Zeiss Microlmaging GmbH, Göttingen, Germany), and photographed with a digital camera (Infinity1-5C, Lumenera Corporation, Ottawa, Canada) at 100× magnification under UV light. The settings were adjusted to yield a good quality image using a software called Infinity Capture Application (Version 6.0.0, Lumenera Corporation Ottawa, Canada).

Analysis of vessel length and diameter

Vessel diameter

Image analysis software (WinCELL 2013; Regent Instruments Inc.) was used to measure the cross-sectional area, A_v, of every rubber-filled vessel in about one-third of the area in *Populus* and *Acer*, and whole cross section of *Quercus* and *Vitis*. Subsamples were based on pie-shaped wedges following the lines of ray cells were selected that include at least 1000 vessels. Three or four wedges were sampled around all 'compass' directions of the stem cross section. Because *Vitis* and *Quercus* have fewer vessels per unit area than the other species, the vessel of the whole section was measured. Equivalent circular diameters were computed from A_v, assuming a circle of equal area $D_v = (4A_v/\pi)^{1/2}$.

Vessel length

Following the example of Cai et al. (2010), the algorithm used was to count the number of rubber-injected vessels, n, per unit cross-sectional area, A: $N = n/A$. Then, the plot of $\ln(N)$ versus distance from the injection surface (x) was used to compute a slope. λ_v. The vessels are assumed to come to an end in proportion to the number of open vessels, this assumption results in a theoretical exponential extinction of vessel ends given by the following:

$$N = N_0 \exp(\lambda_v x), \tag{2}$$

where N_0 is the number of filled vessels (open to rubber-filling) at $x = 0$, and N is the number at $x > 0$ and λ_v is a fitting coefficient (negative slope); hence, a natural log transform plot can be used to estimate λ_v. As pointed out by (Cohen et al. 2003), the second derivative of Eq. (1) gives the probability distribution function, PDF, previously quoted in the introduction:

$$P_x = x\lambda_v^2 \exp(\lambda_v x), \tag{1}$$

where P_x is the probability of vessels of length x, the most common vessel length, i.e., the mode is given by $-1/\lambda_v$ and the mean vessel length is $\bar{L} = -2/\lambda_v$.

Equations (1) and (2) have been used to compute mean vessel length regardless of vessel diameter in many papers since 2003. A modified algorithm was used to take into account the impact of vessel diameter on vessel length. The modified computational algorithm assumed that vessels in a given size class maintain approximately constant diameter over their entire length. Using a standard Microsoft Excel function, the vessel widths were divided into bins based on size classes of diameter, and the counts of the number of rubber-injected vessels in each size class per unit area (N_c)

were used for the plots of $\ln(N_c)$ versus x. The total number of vessels, N_T, in a size class in the sampled area, A_s, was computed from $N_T = A_s N_c$ Whenever N_T was less than 36, the size class was excluded from further analysis. The reason for the choice of 36 was because the coefficient of variation on random vessel ending is equal to the inverse square root N_T or 1/6, which is a tolerable limit of uncertainty for a point in a linear regression. The bin diameter in size ranges were 5 μm wide for *Acer*, 10 μm wide (e.g., 20–30 or 30–40 μm) for *Quercus* and *Populus*, and 30 μm wide for *Vitis*. In plots involving bin-size class on the x-axis, the value plotted for the abscissa was the middle of the size class, e.g., for a bin from 20 to 30 μm, the bin size was a point at 25 μm and diameter was given the symbol D_v.

Statistical methods

Statistical analysis of the comparison of mean diameter at each distance were done with the SPSS 18.0 statistic package for personal computer (SPSS) using the $P \leq 0.05$ significant level. Comparisons more than two groups between all means were done with one-way ANOVA and the Duncan test. Others linear and two parameter non-linear regressions were obtained using Microsoft Excel to evaluate whether trends were significantly different from zero slope.

Results

Log-linear plots for all vessels regardless of diameter are represented in Fig. 1; shown are plots of $\ln(N)$ versus distance, x, from the injection surface. The slopes of these regressions yielded λ_v from Eq. (1), and mean vessel length in all vessels regardless of D was computed from $\bar{L} = -2/\lambda_v$.

Figure 2 gives typical plots of natural log of vessel count versus distance from the injection surface for the bin diameter size classes, N_c, shown in the legend. In each
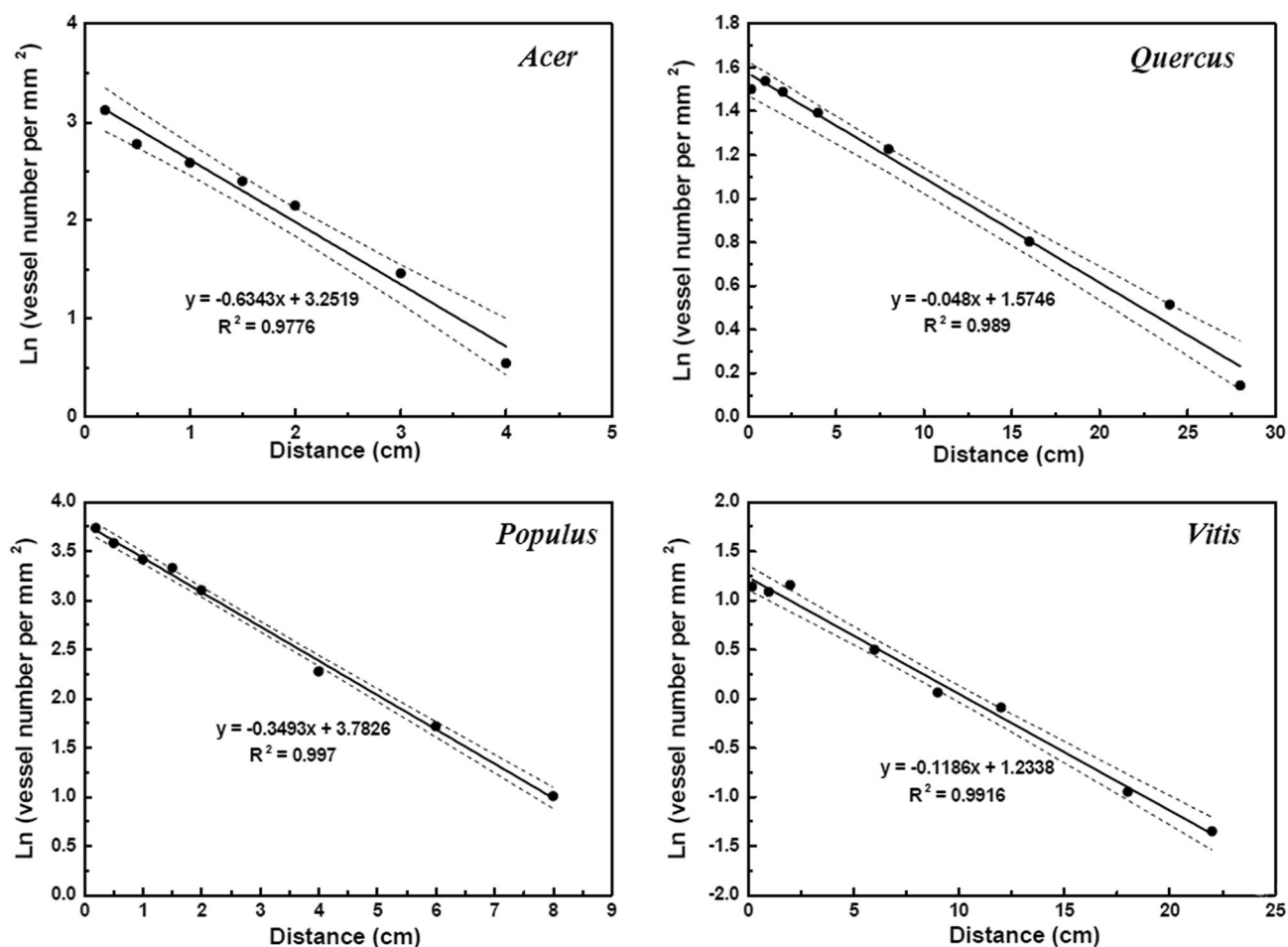
Fig. 1 Examples of natural log-transformed plots of vessel count per unit area versus distance from the injection surface. These are the standard plots used to compute mean vessel length without reference to vessel diameter. Vessel length is equal to −2/slope. *Dash lines* are confidence interval (95%). The slopes of regression lines are used to evaluate λ_v in Eq. (1) for vessels regardless of diameter size class
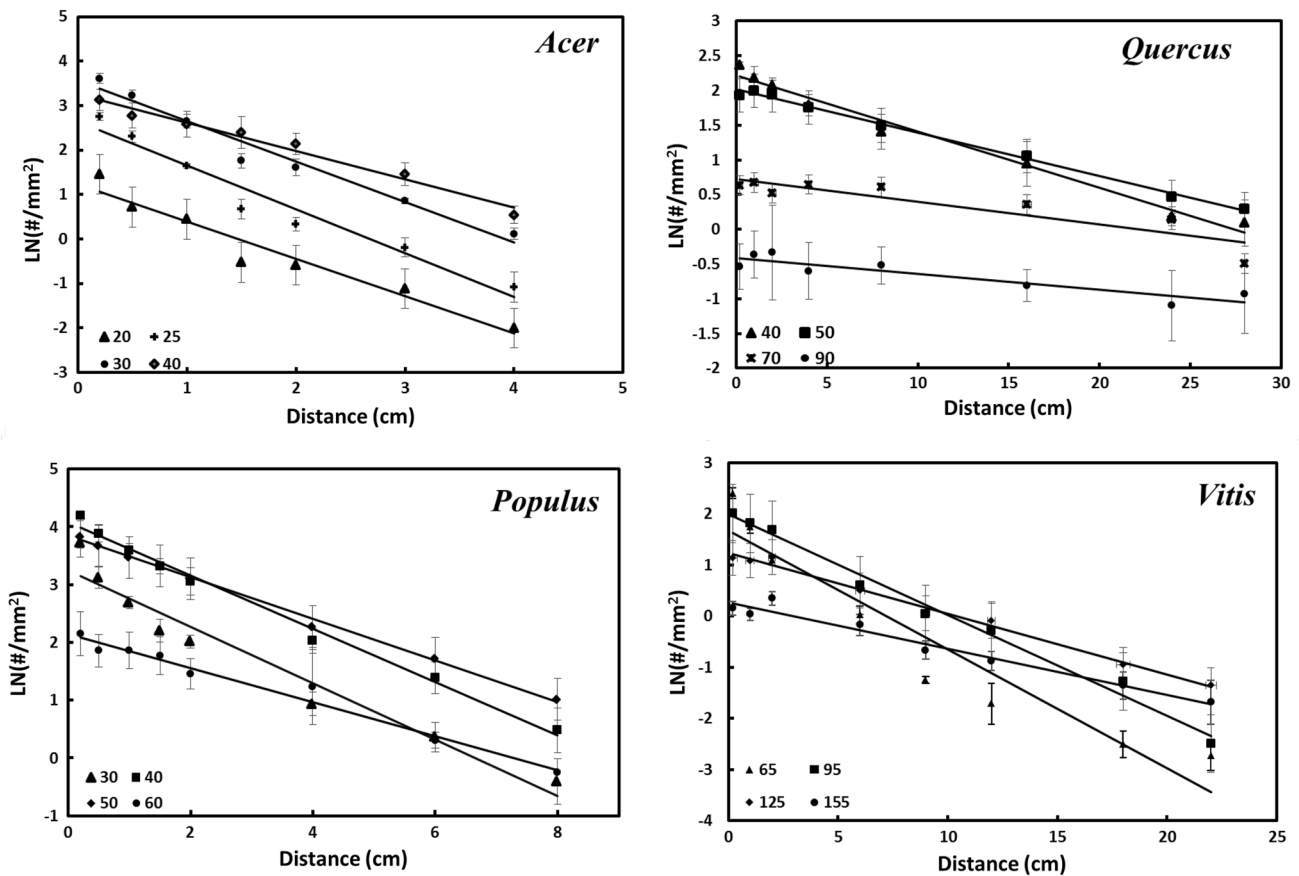
Fig. 2 Four examples at different bin sizes of natural log-transformed plots of vessel count per unit area in a diameter size class versus distance from the injection surface. Shown are means and stand error of counts in five stems for *Acer, Populus, Quercus, Vitis*. The slope of these lines is used to evaluate λ_v in Eq. 1 for each vessel diameter size class. *Error bars* represent one SE ($n = 5$)

graph, four typical regressions are shown. When the regressions are divided into size classes, the *y*-intercepts of the regressions can be interpreted as the maximum number of vessels per unit area of stem cross section in each size class at the injection surface. The count per unit cross-sectional area, N_c, of the rubber-filled vessels decreased with the distance from the injection surface with different slopes. The slope of the narrower vessels was steeper than the slope of the wider vessels. Thus, according to $L_v = -2/\lambda_v$, the average length of the wide vessels was longer than the average length of narrow vessels. All size classes fit linear regressions with an $R^2 > 0.92$, and the sum of all linear regressions in theory should also be linear and should equal the plots shown in Fig. 1.

The next two figures showed clear evidence that wider vessels were longer vessels and that the mean diameter of rubber-injected vessels increased with the distance from the injection point. This provided additional experimental proof that the analysis algorithm was valid.

Figure 3 is a plot of the frequency distribution (PDFs) of vessel diameter actually measured at different distances from the rubber-injection surface. In all cases, at a longer distance from the injection surface, the percentage of wide vessels was larger than that of the shorter distance, which means that the longer vessels tend to be the wide vessels. In addition, the mode (maximum frequency) shifted to larger diameters as the distance from the rubber-injection point increased. This provided a necessary but not sufficient proof that mean vessel diameter of rubber-injected vessels ought to increase with distance from the injection surface.

An additional verification of the computational algorithm was that mean diameter increased with distance from the injection surface, as shown in Fig. 4. The black bars for *Quercus* and *Vitis* give the mean vessel diameter of all rubber-filled vessels. When the letters above the bars are different for different bars, it means that the means are significantly different. The colored stacked bars also give mean vessel diameter of all rubber-filled vessels. The different colors in the stacks show how much each bin diameter contributes to the mean. Colors from the top to the bottom of the bars were ranked from largest bin diameter to smallest. The numbers at the top of the colored
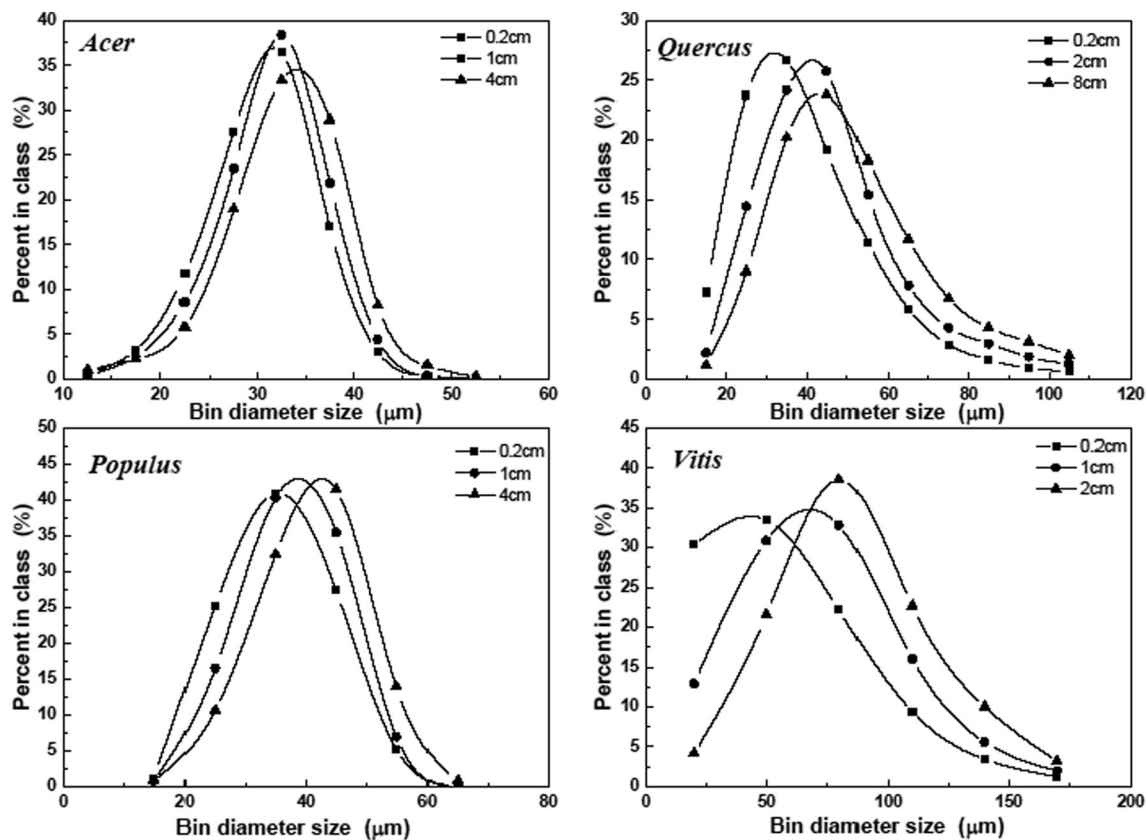
Fig. 3 Frequency distribution of vessel diameters plotted as percentage of vessels (y-axis) in each bin diameter size class (x-axis). Points are a plot of the average percentage of rubber-filled vessels in each diameter size class for five stems on the x-axis. The frequency distributions were computed at different distances from the injection surface as shown in the legend of each graph

bars give the total number of vessels that were rubber filled at the distance on the x-axis. The widest bin diameters contributed more to the mean value as the distance from the injection surface increased. It can also be seen that the smallest bin diameters contributed less to the mean value as the distance from the injection surface increased.

The results in Figs. 3 and 4 were consistent with the algorithm advanced in the methods section to compute vessel length versus vessel diameter, as shown in Fig. 5. All the plots in Fig. 5 had slopes that were significantly different from zero. Plots appear linear and have high R^2 values. The slopes suggested that in all species, vessel length increased with vessel diameter, and that this dependence on diameter was highly significant in these four species ($P < 0.002$). The values of mean vessel length and mean vessel diameter computed by the air injection method and rubber-injection method (Pan et al. 2015) fell within the range of mean vessel length and mean vessel diameter for each species, but as explained in Pan et al. (2015), the air injection means tended to be weighted towards the length of larger diameter vessels.

Discussion

Ewers et al. (1990) examined the maximum vessel diameter and found that it correlated linearly with maximum vessel length among species of woody vines and shrubs ($R^2 = 0.62$; $P = 0.001$). Hacke et al. (2006) had summarized between-species values (28 species) of $\bar{L}$ and $\bar{D}$, and showed that a plot of log ($\bar{L}$) versus log ($\bar{D}$) has a slope of 1.48 and $R^2 = 0.63$. Other studies have found that $\bar{D}$ and $\bar{L}$ are traits that were linked closely to vulnerability to embolism (Lens et al. 2011).

Cai et al. (2010) were the first to develop a protocol for determining how vessel length, L_v, depended on D_v within the genus *Populus*, in a study including *Populus tremuloides* and two hybrids of *Populus* cv. P38P38 (*P. balsamifera* × *P. simonii*) and cv. Northwest (*P. deltoides* × *P. balsamifera*). Our results in Fig. 5 are more convincing than Cai's research, because results in our paper differ in the magnitude of the dependence. The average slope of Cai's results was from 0.03 to 0.06 cm μm^{-1} but in our studies, the slopes were much steeper. The slopes ranged from 0.09 to 0.80 cm μm^{-1}
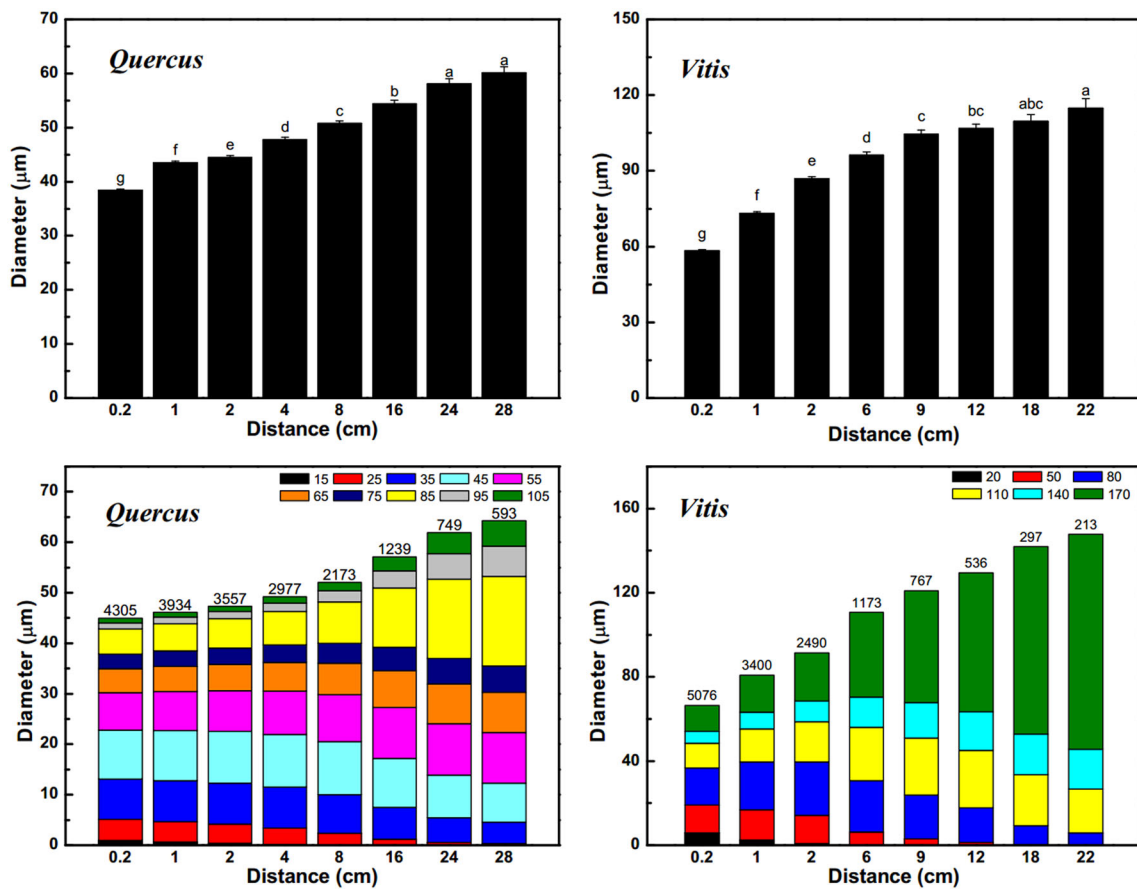
Fig. 4 Mean vessel diameter of rubber-filled vessels versus the distance from the rubber-injection surface. *Upper figures* show the mean diameter at each distance based on raw data. Diameter having a *letter* in common are not significantly different at $P = 0.05$. *Lower figures* represent the predicted vessel diameter based on the regression equation from natural log-transformed plot for each bin-size diameter. The *color* of each stack bar stands for the contribution of each bin size to mean diameter at each distance. *Error bars* represent one SE (n = vessel number at each distance)

with the smallest dependence found in *Populus* cv. 84K to the largest found in *Quercus*. The higher slopes in our studies revealed much stronger dependencies of vessel length on bin diameter size class than the previous study. The dynamic range of vessel lengths was also more in our study. Defining dynamic range as the ratio of longest-to-shortest vessel length, the biggest dynamic range was 11:1 in *Quercus* and the smallest was 2.5:1 in *Acer*. In contrast, the dynamic ranges were much smaller in Cai et al. (2010), that was 2.3:1 down to 1.12:1. The dramatic differences between species are made more evident by plotting all lines on the same *x*- and *y*-scales, as shown in Fig. 6. *Quercus* and *Vitis* have much larger dynamic ranges than the other species in Fig. 6.

The other new contribution of this paper was to test hypotheses that logically followed from the computation algorithm used. It was assumed that vessel diameter is relatively constant over the length of the vessel. If narrow diameter vessels are short vessels and if wide diameter vessels are long vessels, then the following predictions

follow that the mean vessel diameter of rubber-filled vessels should increase with distance from the injection surface, and this was proved the bar histograms in Fig. 4. In addition, the contribution of small diameter vessels to the mean diameter should decline with distance from the injection surface, and the contribution of large diameter vessels to the mean diameter should increase with distance from the injection surface. These predictions were confirmed by the stacked bar histograms in Fig. 4. Finally, the frequency distribution of vessel diameters versus bin diameter should shift to higher bin values as the distance from the injection surface increased. This was confirmed by Fig. 3.

The reader should note that the mean vessel diameters, which are equal to the height of the colored bars, differ slightly from the black bars. This was because of differences of calculation technique between the black and colored bars. In the black bars, the mean values were computed from the mean of all vessels measured in the digital images at 0.2 mm from the injection surface. In the
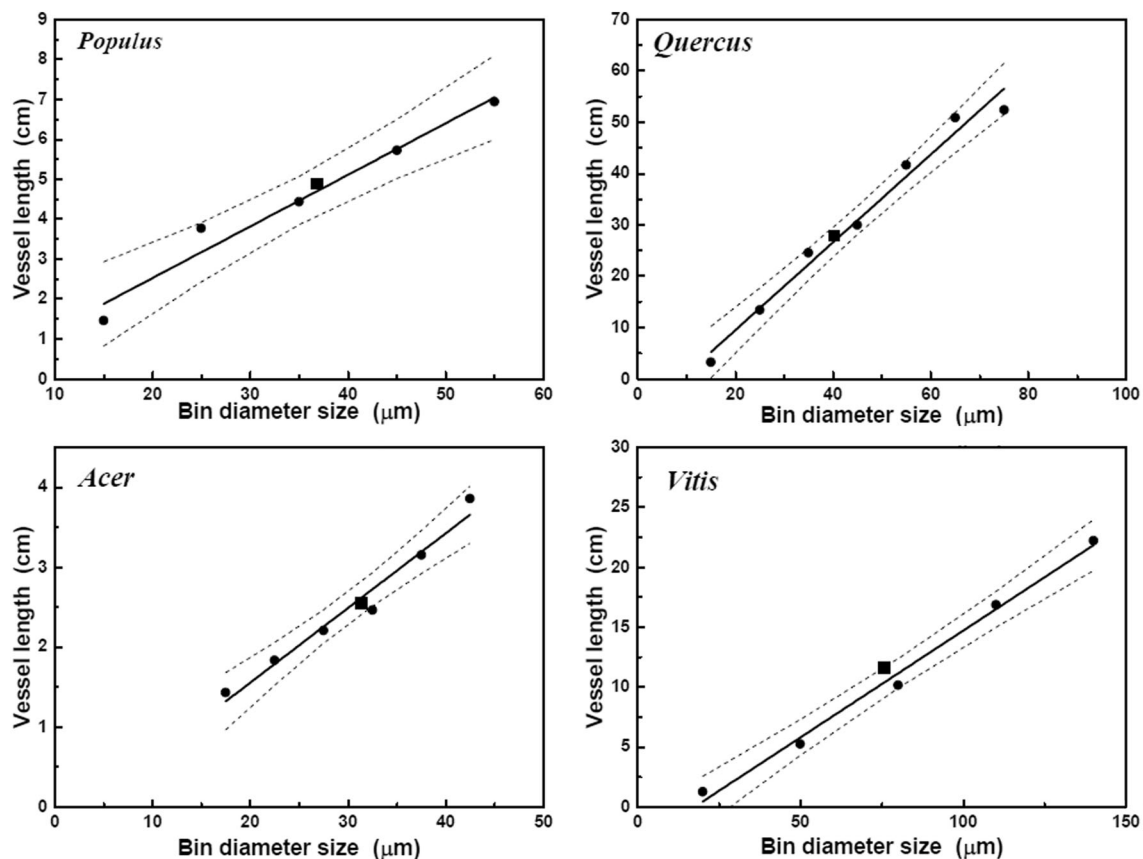
Fig. 5 Mean vessel length in a diameter size class, L_{mean} versus diameter size class is shown for four species. The *squares* represent the mean length plotted, $\bar{L}$, versus mean vessel diameter, $\bar{D}$, of each species from Fig. 1 were all size classes are pooled into one plot. *Dashed lines* represent the confidence interval (95%). The *dots* are L_v values based on the bin size class of vessels. The regressions are: *Acer*: $L_v = 0.0934\ D_v - 0.5475$ ($R^2 = 0.9679\ P = 0.0003$); *Populus*: $L_v = 0.1291\ D_v - 0.7007$ ($R^2 = 0.9683\ P = 0.002$); *Quercus*: $L_v = 0.7972\ D_v - 7.6125$ ($R^2 = 0.9713\ P = 4.80067\text{E}-05$); *Vitis*: $L_v = 0.1783\ D_v - 5.793$ ($R^2 = 0.9923\ P = 0.0002$)

colored bars, the mean vessel diameters were computed from all of the regression lines like those in Fig. 2 extrapolated to zero distance. It can be argued that regression lines give a better estimate of the population mean number of vessels in a bin diameter class versus distance from the injection surface. The y-axis in Fig. 2 is the natural log of the number of vessels per mm^2 of wood. Therefore, the total number of vessel, N_T, was computed from the anti-log times the cross-sectional area of the wood in mm^2 of each cross section. Then, N_T times the vessel diameter at the middle of each size class was used to compute the contribution to the mean for each stacked color in the multi-color bar. The calculations were also done from actual measured values in each bin-size class, and in this case, the peak of the black bars equaled the peak of the stacked colored bars (data not shown). There were only slight qualitative differences in the relative contributions of the bin-size classes (each color bar-height) to the multi-colored stacked bar when direct measurements were made (data not shown).

There is very little direct anatomical evidence for how vessels change in diameter from microscopy, because a microscope is far too myopic to visualize vessel dimension over distances exceeding about 0.5 mm in longitudinal sections. Part of the problem is that vessel rarely remains in a thin section (single slice) of a radial or tangential section of stems. However, sequential cross sections photographed by a cinemagraph technique (Zimmermann 1971) can reveal three-dimensional structures based upon films photographed frame by frame from thousands of sequential cross sections of wood. The technique used by Zimmermann required thousands of hours of sectioning and mounting of sections on microscope slides, and it required custom fabricated microtomes and microscopes. The microtome had to be modified to advance stems many cm long to the cutting blade in 20–40 μm increments. A dual-stage microscope with mirrors and a single ocular had to be fabricated to manipulate microscope slides by rotation and by x–y-manipulation to superimpose images for sequential photographs on 16 mm films. Hence, there are only a few

Fig. 6 This is a summary of vessel length versus diameter of the four species in this paper and two species from Cai et al. (2010). Plotting all the values on one axis reveals the dramatic differences between species. NW is the clonal hybrid Northwest (*Populus deltoides* × *Populus balsamifera*) and Aspen is *Populus tremuloides* Michx
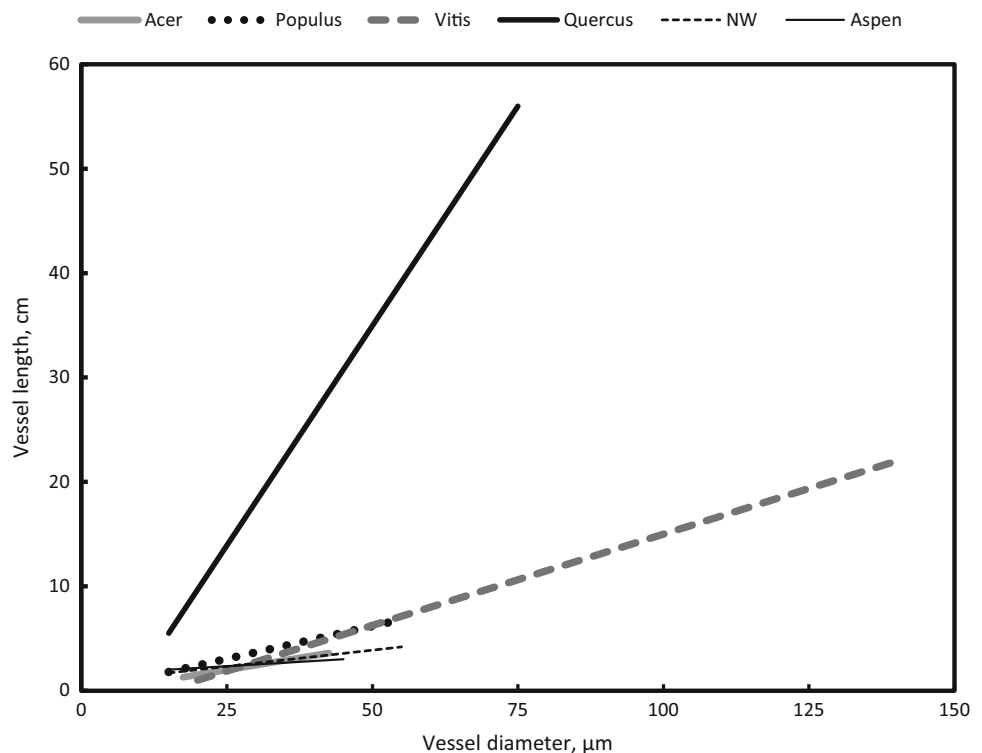
extant examples available; for example, Fig. S1 reproduced from Tyree and Zimmermann (2002). A few examples can be seen of invariant vessel diameter over long distances. Without the aid of a ruler, it is obvious that vessel numbers 22 and 26 in Fig. S1 are narrower than all other vessels. With the aid of a ruler, it can also be seen that vessel number 16 is the widest vessel in Fig. S1. In addition, a ruler can be used to reveal that any given vessel diameter is approximately constant along the visible length of all vessels in Fig. S1.

With modern digital photography and digital image analysis software, the task could be completed faster, without a dual-stage microscope and 16-mm filming, but a custom fabricated microtome is still required. However, we are not aware of any modern studies.

Long and wide vessels dominate the theoretical hydraulic conductivity of stems. The theoretical hydraulic conductivity can be equated to the sum of the diameters of vessels to the fourth power, which follows from the Hagen–Poiseuille law. From Fig. 5, the mean vessel length (square symbol) for *Quercus* and *Vitis* occurred in vessel that was about 40 and 75 μm in diameter, respectively. In *Quercus*, the number of vessels ≥40 μm in diameter was equal to 27.5% of all those vessels but accounted for 90.8% of the theoretical hydraulic conductivity. In *Vitis*, the number of vessels ≥75 μm was equal to 36.9% of all those vessels but accounted for 91.3% of the theoretical hydraulic conductivity. Therefore, more work needs to be

done to understand the functional significance of long and wide vessels, because they may account for most of the hydraulic conductivity of stems.

The results in this paper also suggest that a re-evaluation of concepts of optimal vessel design might be appropriate (Hacke et al. 2006; Sperry et al. 2007; Lens et al. 2011). Detailed discussion is beyond the scope of this paper, but briefly, the key points are worth summarizing. Optimization of vessel conductance is often assumed to happen with vessel lumen conductance equals the vessel-to-vessel conductance (across pit membranes). However, increased contact area through pits is at the risk of increased vulnerability of embolism through 'rare pits', i.e., the rare pit membrane with a large pit pore that will seed embolisms during water stress. So far, analysis of these factors has been based on species means for vessel diameter, length, and contact area. The problem is that species means may not represent the hydraulically important vessels in species with large dynamic ranges of diameter and length such as *Vitis* and *Quercus* in Fig. 6. Future work needs to be focused on the dependence on vessel diameter on contact area, which is a topic that has been unaddressed in the past literature. Once this is known, a review of optimization theory may be appropriate.

topic, provided training, suggested methods of data analysis, and contributed mostly to writing.

References

Cai J, Tyree MT (2010) The impact of vessel size on vulnerability curves: data and models for within-species variability in saplings of aspen, *Populus tremuloides* Michx. Plant Cell Environ 33:1059–1069

Cai J, Zhang S, Tyree MT (2010) A computational algorithm addressing how vessel length might depend on vessel diameter. Plant Cell Environ 33:1234–1238

Cohen S, Bennink J, Tyree MT (2003) Air method measurements of apple vessel length distributions with improved apparatus and theory. J Exp Bot 54:1889–1897

Ewers FW, Fisher JB, Chiu S-T (1990) A survey of vessel dimensions in stems of tropical lianas and other growth forms. Oecologia 84:544–552

Hacke UG, Sperry JS, Wheeler JK, Castro L (2006) Scaling of angiosperm xylem structure with safety and efficiency. Tree Physiol 26:689–701

Jacobsen AL, Pratt RB, Tobin MF, Hacke UG, Ewers FW (2012) A global analysis of xylem vessel length in woody plants. Am J Bot 99:1583–1591

Lens F, Sperry JS, Christman MA, Choat B, Rabaey D, Jansen S (2011) Testing hypotheses that link wood anatomy to cavitation resistance and hydraulic conductivity in the genus *Acer*. New Phytol 190:709–723

Pan R, Geng J, Cai J, Tyree MT (2015) A comparison of two methods for measuring vessel length in woody plants. Plant Cell Environ 38:2519–2526

Sperry JS, Hacke UG, Feild TS, Sano Y, Sikkema EH (2007) Hydraulic consequences of vessel evolution in angiosperms. Int J Plant Sci 168:1127–1139

Tyree MT, Zimmermann MH (2002) Xylem structure and the ascent of sap. Springer, Heidelberg

Zimmermann MH (1971) Dicotyledonous wood structure made apparent by sequential sections. Film E 1735 Institut für den Wissenschaftlichen Film, Göttingen

Zimmermann MH, Brown CL (1971) Trees: structure and function. Springer, Berlin, p 336